Wideband multilayer dual circularly-polarised antenna for array application

Q. Luo✉, S. Gao and L. Zhang

A wideband multilayer antenna with dual circular polarisations (CPs) is presented. The antenna consists of stacked square patches fed by striplines and a branch line coupler. Two orthogonally positioned H-shaped slots are used as the coupling aperture for the striplines. The dual-CP radiation is obtained by exciting the TM_{01} and TM_{10} modes of the radiating element with 90° phase differences. The presented dual-CP antenna has a multilayer configuration with a compact size and it is suitable to be applied to the design of array antennas. To verify this design concept, one prototype operating in the K-band is designed and fabricated. The measurement results show that the prototype has more than 13% impedance bandwidth with good CP radiations.

Introduction: Circularly-polarised antennas have been widely used in satellite communications because of their advantages which include reducing multipath fading and robustness to the misaligned orientations between transmitters and receivers [1]. A recent study [2] showed that by exploiting the polarisation diversity at both the transmitter and receiver, the channel capacity of a single satellite, where it does not have the necessary antenna spacings that are required by multiple-input multiple-output (MIMO) theory to provide a high degree of channel decorrelation, can be significantly improved. To date, there have been few reports in the literature on wideband dual-CP antenna design, especially for array antenna applications. An X-band dual-CP antenna array was presented in [3]. The dual-CP was realised using a branch coupler connected with two probes to feed the square patch. However, the isolation between the left-hand circular polarisation (LHCP) and right-hand circular polarisation (RHCP) ports was not addressed in this paper. A dual-CP waveguide antenna was presented in [4]. This antenna is an open-ended waveguide integrated with a septum polariser and by exciting different modes in the waveguide, either LHCP or RHCP can be obtained. Yet, the waveguide has the disadvantage of bulky size.

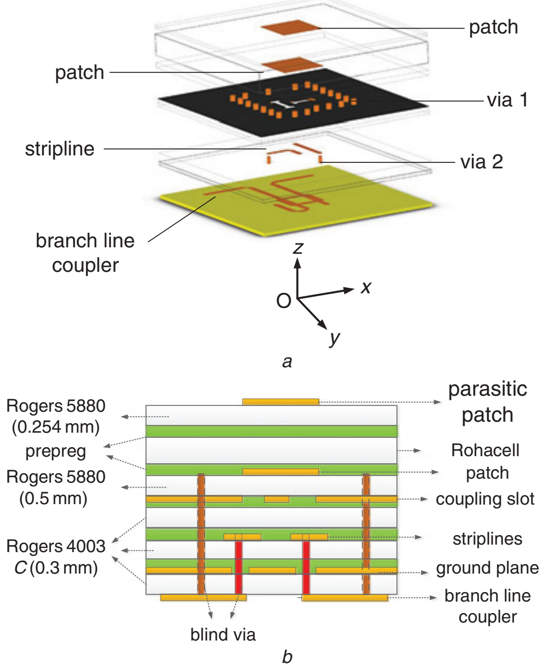

Fig. 1 *Exploded and side view of proposed wideband dual-CP antenna*
a Exploded view
b Side view

The objective of this reported work was to design a wideband dual-CP antenna that can be used as the unit cell for the array antenna design. The proposed design approach is to employ a multilayer configuration and use stacked square patches as the radiating element to improve the bandwidth of the antenna. CP radiation is obtained by feeding the microstrip patch using two orthogonally positioned aperture-coupled striplines. The striplines are incorporated with a branch line coupler, thus the TM_{01} and TM_{10} modes of the radiating element with 90° phase differences can be excited. The proposed antenna has a compact size due to the multilayer configuration so it is suitable for the design of array antennas without any resulting grating lobes. Meanwhile, there is no buried vias used, which simplifies the fabrication complexity normally encountered during the multilayer PCB manufacture process. The presented design approach can be applied to the design of other wideband dual-CP antennas operating at different frequency bands.

Antenna configuration: The configuration of the proposed wideband dual-CP antenna in the K-band is shown in Fig. 1. As can be seen, the radiating element is a dual-feed stacked square patch. The parasitic square patch has a side length of 4.1 mm and is printed on a 0.25 mm-thick Rogers 5880 substrate ($\varepsilon_r = 2.2$, $\tan\delta = 0.0009$). The bottom square patch has a side length of 4.2 mm and is printed on a 0.5 mm-thick Rogers 5880 substrate. Between these two patches, there is a 2 mm-thick Rochacell at HF ($\varepsilon_r = 1.04$, $\tan\delta = 0.003$). Two H-shaped slots are orthogonally positioned as the coupling apertures for the striplines, which excite the TM_{01} and TM_{10} modes of the patch antenna. To obtain the dual-CP radiation, the striplines are incorporated with a branch line coupler that is printed on the bottom layer and connected to the striplines through vias (via 2), which were realised by plated holes. By selecting the corresponding port of the coupler, LHCP or RHCP can be obtained. The striplines and the coupler are printed on different 0.3 mm-thick RO4003C substrates ($\varepsilon_r = 3.55$, $\tan\delta = 0.0027$). There are six conductive layers printed on six substrates that are bonded together by prepregs. The total thickness of the antenna is ~3.5 mm.

When used as an array unit cell, the presented antenna including the RF interface can fit in an area with dimensions of less than 12 × 12 mm ($0.75\lambda_{19\ \mathrm{GHz}}$). Therefore, it can be applied to an array antenna design free from any grating lobes within a scan angle range of about ±23° with a triangular lattice. Shielding vias (via 1) are introduced around the radiating element in order to suppress the parallel plating modes as the antenna has multiple conductive layers. It can also improve the isolations between the neighbouring radiating elements when the antenna is used as the unit cell for array application [5].

Simulation and experiment results: One prototype of the proposed wideband dual-CP antenna in the K-band was fabricated and measured. Fig. 2 shows the top and back views of the fabricated prototype. To characterise the radiation performance of the antenna element, two surface mount SMPM connectors were used and the size of the substrate was enlarged in order to provide proper space to solder these surface mount connectors as well as to facilitate the measurement setup.

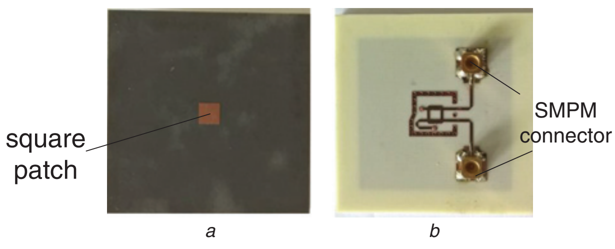

Fig. 2 *Top and back view of fabricated prototype*
a Top view
b Back view

Fig. 3 shows the simulated and measured scattering parameters of the dual-CP antenna. The measurement results suggest that the isolation between two ports is better than 10 dB from 18 to 20.5 GHz (13%), within which the return losses from both ports are higher than 10 dB. At the central frequency, the isolation is about 25 dB. Generally there is good agreement between the measured and simulated results, except that the measured reflection coefficient from port 1 (RHCP port) shows higher amplitude than the simulated one. This is mainly due to the fabrication error and possible misalignment between the PCB layers (e.g. via position), which causes mismatching between the coupler and the striplines. As presented later, due to this mismatch, the axial ratio (AR) of the prototype is also affected.

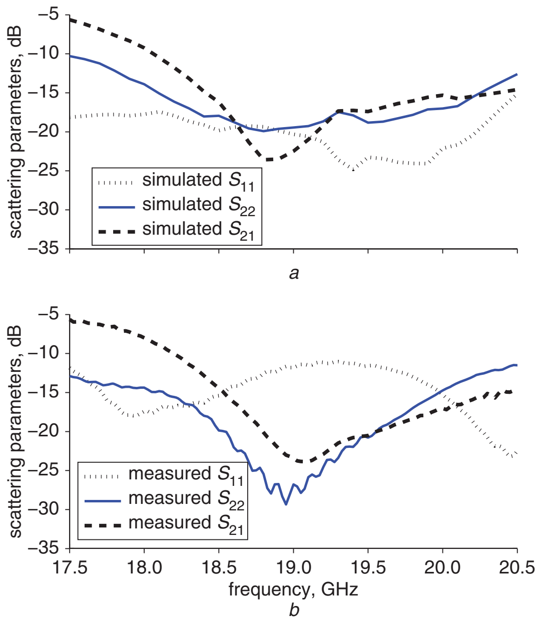

Fig. 3 *Simulated and measured scattering parameters of dual-CP antenna*
a Simulated
b Measured

Fig. 4 presents the simulated and measured AR of the dual-CP antenna when it radiates LHCP waves. It is expected that low AR should be obtained from 17 to 20.5 GHz as suggested by the simulation results. However, as explained above, due to the mismatching between the coupler and the striplines caused by the possible fabrication errors, the measured AR is higher than the simulation results, especially at the lower frequency range. Fig. 5 presents the measured LHCP radiation patterns of the presented dual-CP antenna. It is found that it has low cross-polarisation at the broadside. Similar results were also observed when the RHCP ports were excited. These results are not shown in this Letter due to limited space.

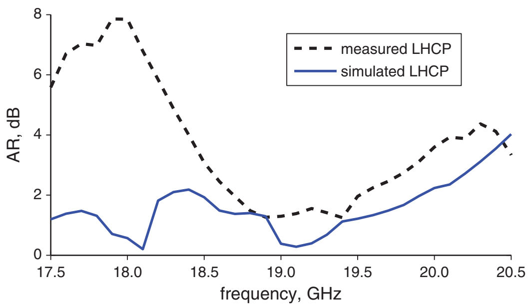

Fig. 4 *Simulated and measured AR of dual-CP antenna when it radiates LHCP waves*

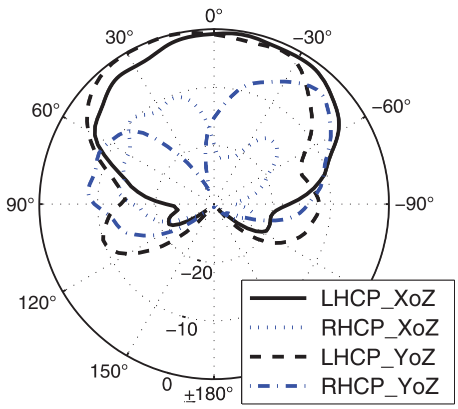

Fig. 5 *Measured radiation patterns of presented antenna when it radiates LHCP waves at 18.5 GHz*

Fig. 6 presents the simulated gain and radiation efficiency when the proposed antenna radiates LHCP and RHCP waves. It shows that it has stable gain (4.9 dBic) and radiation efficiency better than 85% within its entire operation bandwidth.

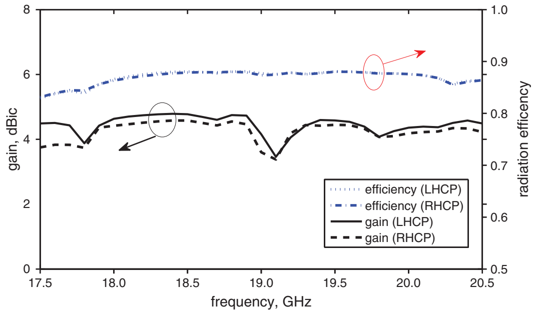

Fig. 6 *Simulated gain and radiation efficiency of presented antenna when it radiates LHCP and RHCP waves*

Conclusion: A wideband dual-CP antenna is presented in this Letter. It has a compact size with a multilayer structure and can be used either as an individual antenna or as a unit cell for the design of array antennas. One prototype operating in the K-band is designed, fabricated and measured. Experimental results show that the presented antenna has more than 13% impedance bandwidth with good circular polarisation. The presented design approach can be applied to the design of wideband dual-CP antennas operating at other frequency bands. Future work will include further optimising the antenna design with better fabrication tolerances, refabricating the prototypes, and designing a direct radiating array antenna using the presented antenna element.

Acknowledgment: The authors are grateful for funding from the EC FP7 GaNSat project, contract number 606981.

Submitted: *25 September 2015* E-first: *5 November 2015*
doi: 10.1049/el.2015.3343
One or more of the Figures in this Letter are available in colour online.

Q. Luo, S. Gao and L. Zhang (*School of Engineering and Digital Arts, University of Kent, Canterbury, United Kingdom*)

✉ E-mail: qiluo@ieee.org

References

1 Gao, S., Luo, Q., and Zhu, F.G.: 'Circularly polarized antennas' (Wiley-IEEE Press, 2014)
2 Arapoglou, P., Liolis, K., Bertinelli, M., Panagopoulos, A., Cottis, P., and De Gaudenzi, R.: 'MIMO over satellite: a review', *IEEE Commun. Surv. Tutor.*, 2011, **13**, pp. 27–51
3 Garcia-Aguilar, A., Inclan-Alonso, J., Vigil-Herrero, L., Fernandez-Gonzalez, J., and Sierra-Perez, M.: 'Low-profile dual circularly polarized antenna array for satellite communications in the X band', *IEEE Trans. Antennas Propag.*, 2012, **60**, pp. 2276–2284
4 Kumar, C., Srinivasan, V., Lakshmeesha, V., and Pal, S.: 'Novel dual circularly polarized radiating element for spherical phased-array application', *IEEE Antennas Wirel. Propag. Lett.*, 2009, **8**, pp. 826–829
5 Luo, Q., Gao, S., Zhang, C., Zhou, D., Chaloun, T., Menzel, W., Ziegler, V., and Sobhy, M.: 'Design and analysis of a reflect array using slot antenna elements for Ka-band SatCom', *IEEE Trans. Antennas Propag.*, 2015, **63**, pp. 1365–1374